Weak localization and weak antilocalization in doped germanium epilayers

P. J. Newton, R. Mansell, S. N. Holmes, M. Myronov, and C. H. W. Barnes

Citation: Appl. Phys. Lett. **110**, 062101 (2017); doi: 10.1063/1.4975600
View online: http://dx.doi.org/10.1063/1.4975600
View Table of Contents: http://aip.scitation.org/toc/apl/110/6
Published by the American Institute of Physics

Weak localization and weak antilocalization in doped germanium epilayers

P. J. Newton,[1,a)] R. Mansell,[1] S. N. Holmes,[2] M. Myronov,[3] and C. H. W. Barnes[1]
[1]*Department of Physics, Cavendish Laboratory, University of Cambridge, J. J. Thomson Avenue, Cambridge CB3 0HE, United Kingdom*
[2]*Toshiba Research Europe Limited, Cambridge Research Laboratory, 208 Cambridge Science Park, Milton Road, Cambridge CB4 0GZ, United Kingdom*
[3]*Department of Physics, University of Warwick, Coventry CV4 7AL, United Kingdom*

(Received 12 December 2016; accepted 23 January 2017; published online 7 February 2017)

The magnetoresistance of 50 nm thick epilayers of doped germanium is measured at a range of temperatures down to 1.6 K. Both n- and p-type devices show quantum corrections to the conductivity in an applied magnetic field, with n-type devices displaying weak localization and p-type devices showing weak antilocalization. From fits to these data using the Hikami-Larkin-Nagaoka model, the phase coherence length of each device is extracted, as well as the spin diffusion length of the p-type device. We obtain phase coherence lengths as large as 325 nm in the highly doped n-type device, presenting possible applications in quantum technologies. The decay of the phase coherence length with temperature is found to obey the same power law of $l_\phi \propto T^c$, where $c = -0.68 \pm 0.03$, for each device, in spite of the clear differences in the nature of the conduction. In the p-type device, the measured spin diffusion length does not change over the range of temperatures for which weak antilocalization can be observed. The presence of a spin-orbit interaction manifested as weak antilocalization in the p-type epilayer suggests that these structures could be developed for use in spintronic devices such as the spin-FET, where significant spin lifetimes would be important for efficient device operation. *Published by AIP Publishing.*
[http://dx.doi.org/10.1063/1.4975600]

The recent works on spin transport in germanium have shown it to be an ideal candidate for use in spintronic technologies.[1–11] In germanium, the Dyakonov-Perel spin relaxation mechanism is suppressed by the inversion symmetry of the germanium crystal and the influence of the hyperfine interaction is minimal because of the zero nuclear spin of germanium's most abundant isotopes.[12–14] Doped epilayers are a useful system on which to investigate spin transport in germanium, owing to the relatively simple magnetotransport properties when compared to quantum well structures that are often found to display parallel conduction effects or require illumination to excite charge carriers.[4,15,16]

For the realisation of spintronic devices such as the spin-FET, the development of a semiconductor channel with a long spin diffusion length and where spins can be manipulated by the application of an external field, using the Rashba effect for example, is necessary.[17] A thorough comparison of n-type and p-type epilayers is therefore useful to analyse their possible applications in the spintronic and quantum devices.

In this paper, we perform a low temperature magnetotransport study of Hall bars containing either p- or n-type germanium epilayers. We observe weak localization and weak antilocalization in the n-type and p-type magnetotransport, respectively. By analysing fits to these data, we are able to extract the temperature dependence of the phase coherence length and spin diffusion length in these devices.

Schematic diagrams of the structures used in this work are shown in Figures 1(a) and 1(b). Two n-type devices were measured with different doping densities. The n-type structures were grown by reduced pressure chemical vapour deposition (RP-CVD),[11] whereas the p-type devices were made from commercially grown wafers. These structures are designed such that the conducting layer is unstrained and is epitaxial. Hall bars were produced using standard cleanroom techniques. An image of the Hall bar of sample p50 is shown in Figure 1(c). All Hall bars used in this work had the same dimensions.

Magnetotransport measurements were carried out in a perpendicular magnetic field up to 5 T at temperatures as low as 1.6 K. In these Hall bar devices, an alternating current of 100 nA was applied at a frequency of 33 Hz and longitudinal and transverse magnetoresistance measurements made using a lock-in technique.

The variation with temperature of the zero-field resistivity (ρ) of sample n31 is shown in Figure 2. This has the behaviour that is expected of a highly doped semiconductor. As the temperature increases, initially, the resistivity drops as carriers are excited from an impurity band. Above ~30 K, the mobility begins to decrease, owing to the influence of phonon scattering, approaching a $T^{-3/2}$ dependence at 70–90 K. Above ~200 K (not shown), carriers are thermally excited in the Si substrate and the carrier density increases dramatically, reducing the resistivity. The inset of Figure 2 shows how, in the temperature range up to 60 K, the carrier density is approximately constant. All three samples measured in this work show similar characteristics to those shown in Figure 2. The carrier density and mobility of each device at 1.6 K are displayed in Table I.

Figure 3 shows the magnetoresistance and magnetoconductance of device n31 for a range of temperatures, as

a)Author to whom correspondence should be addressed. Electronic mail: pjn32@cam.ac.uk

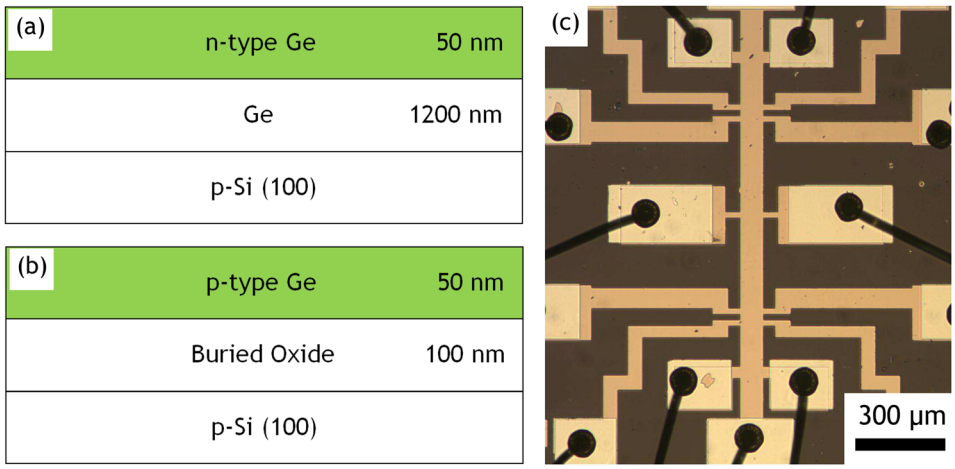

FIG. 1. The layer structures of (a) the n-type and (b) the p-type devices investigated in this work. (c) An optical image of the Hall bar of sample p50.

indicated. The conductance data are formatted as $\Delta G = G(B) - G(0) = \frac{1}{\rho_{xx}(B)} - \frac{1}{\rho_{xx}(0)}$ to show the change in conductivity of the sample relative to the zero field conductivity. The data shown here are averaged from sweeps in the positive and negative sweep directions in order to eliminate any linear drift caused by temperature fluctuations during measurement. Similar data are extracted for the device n29.

Fits to conductivity data for samples with weak localization or weak antilocalization are obtained using the Hikami-Larkin-Nagaoka (HLN) model[18]

$$\Delta G(B)_{HLN} = \alpha \frac{e^2}{2\pi^2\hbar}\left[\psi\left(\frac{1}{2}+\frac{B_\phi}{B}\right) - \ln\left(\frac{B_\phi}{B}\right)\right], \quad (1)$$

where $\psi(x)$ is the digamma function of a physical variable x and α is a constant equal to 1 or $-1/2$ for a single layer exhibiting weak localization or antilocalization, respectively. $B_\phi = \frac{\hbar}{4el_\phi^2}$ is a magnetic field defined by a phase coherence length, l_ϕ. In the limit where the spin-orbit length, l_{SO}, is non-negligible the model becomes

$$\Delta G(B)_{HLN} = \alpha \frac{e^2}{2\pi^2\hbar}\left[\psi\left(\frac{1}{2}+\frac{B_\phi}{B}\right) - \ln\left(\frac{B_\phi}{B}\right) - 2\psi\left(\frac{1}{2}+\frac{B_\phi + B_{SO}}{B}\right) + 2\ln\left(\frac{B_\phi + B_{SO}}{B}\right) - \psi\left(\frac{1}{2}+\frac{B_\phi + 2B_{SO}}{B}\right) + \ln\left(\frac{B_\phi + 2B_{SO}}{B}\right)\right], \quad (2)$$

where $B_{SO} = \frac{\hbar}{4el_{SO}^2}$ is a characteristic magnetic field defined by the spin-orbit length.[18,19] The phase coherence length obtained by these measurements is greater than the thickness of the epilayer, suggesting that this system is quasi-two dimensional and justifying our use of this 2D model. HLN models that contain $B_e = \frac{\hbar}{4el_e^2}$, where l_e is the elastic scattering length, are not used because l_e is sufficiently small that its inclusion has very little impact on the quality of the fit.

When producing the fits shown in Figure 3, a quadratic background is also added to the fit because of the quadratic background from the Lorentz force in the resistivity data, such that

$$\Delta G(B)_{FIT} = \Delta G(B)_{HLN} + CB^2, \quad (3)$$

where C is a constant that depends on the measurement temperature. In the n-type devices, it is found that the spin-orbit length is sufficiently small that the shorter HLN model shown in Equation (1) can be used to fit ΔG.

Similarly, the results of magnetoresistance measurements made on sample p50 are shown in Figure 4. Again, the data are shown as magnetoresistance and as $\Delta G = G(B) - G(0)$ to show the change in conductivity of the sample relative to the zero field conductivity.

Fits to the conductivity data shown in Figure 4 are obtained using the HLN model shown in Equation (2) (the

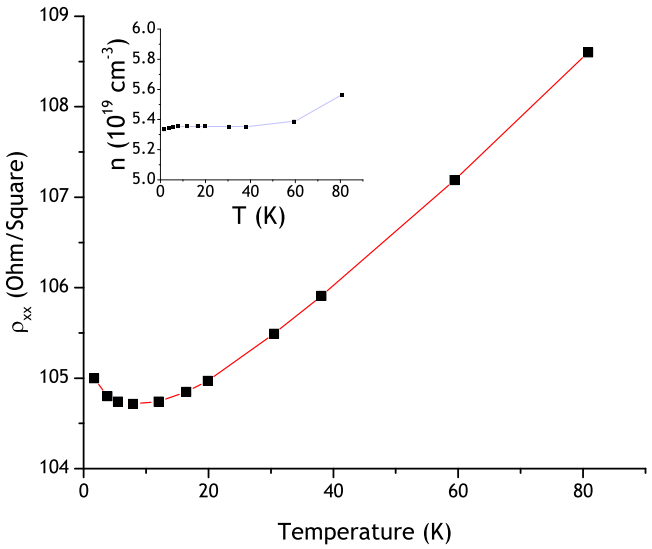

FIG. 2. The temperature dependence of the zero-field resistivity of sample n31. Inset: the variation of the carrier density over the same temperature range.

TABLE I. The carrier density and mobility of each device investigated in this work obtained from Hall measurements at 1.6 K.

Device	Carrier Density (cm^{-3})	Mobility ($cm^2\,V^{-1}\,s^{-1}$)
n29	1.05×10^{19}	345
n31	5.3×10^{19}	220
p50	8.5×10^{18}	200

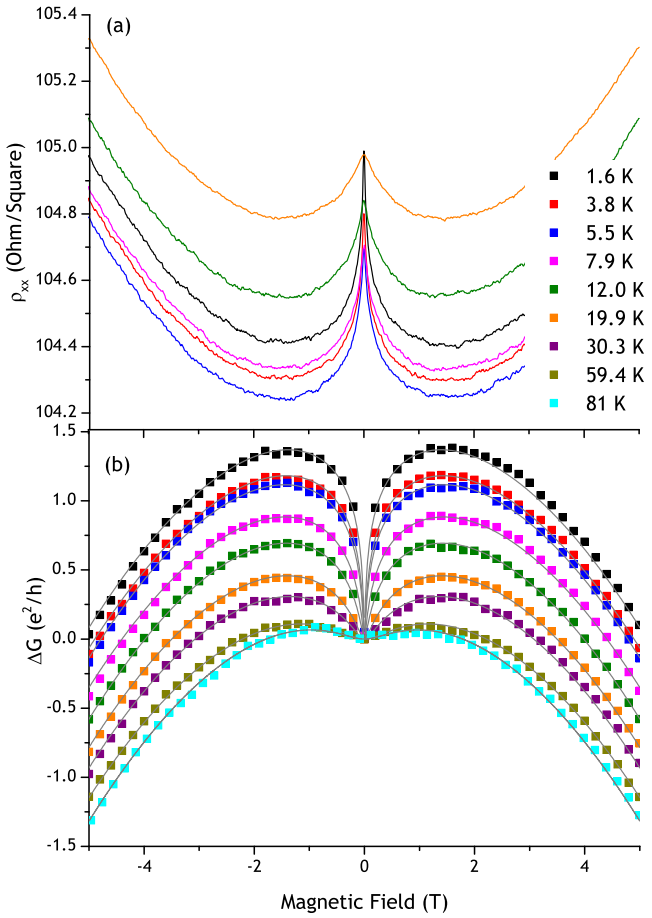

FIG. 3. The (a) magnetoresistance and (b) differential conductivity of sample n31 measured at a range of temperatures. The magnetoresistance data include an arbitrary linear offset for the clarity of presentation. Coloured lines and points are experimental data at the temperatures indicated, and grey lines are fits to weak localization using the HLN model.

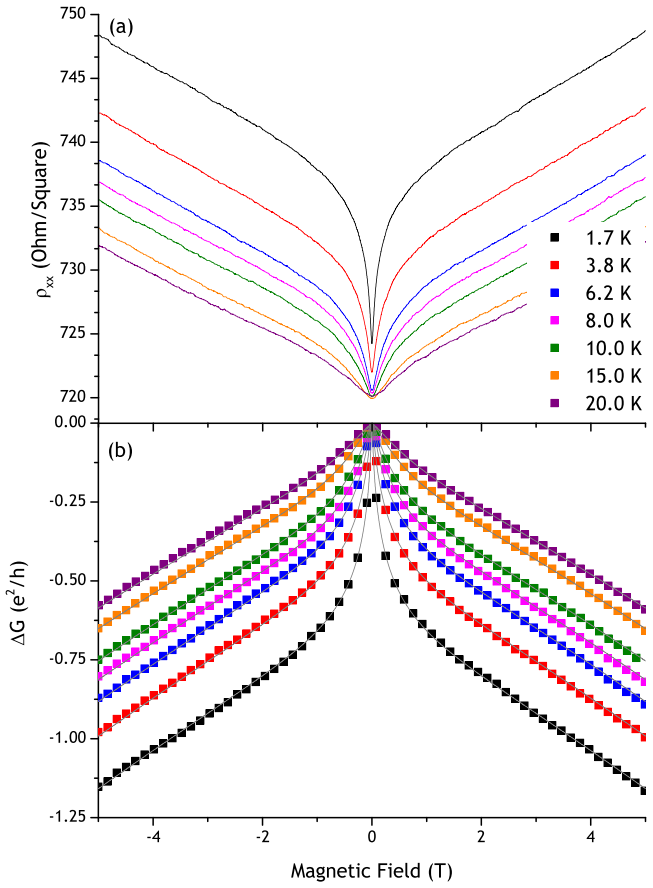

FIG. 4. The (a) magnetoresistance and (b) differential conductivity of sample p50 measured at a range of temperatures. Coloured lines and points are experimental data at the temperatures indicated, and grey lines are fits to weak antilocalization using the HLN model.

spin-orbit length is non-negligible). Since this device contains a single conducting layer that exhibits weak antilocalization, the constant α is fixed to a value of $-1/2$.

It might be expected that these data would have a background that is quadratic in magnetic field, since this is a semiconductor with hole transport in only a single layer.[20] However, the data show a clear linear background at high magnetic fields in contrast to the n-type samples. This behaviour has been observed in other semiconductor systems[21] and at room temperature in germanium devices.[22] It is shown that magnetoresistance can be linear at even very low fields for systems with a large mobility disorder. This is consistent with the data obtained for the p-type sample, since the low temperature mobility in this device has the relatively small value of $200\,\mathrm{cm}^2\ \mathrm{V}^{-1}\ \mathrm{s}^{-1}$.[23] Therefore, in addition to the terms in Equation (2), a linear background is included in the fit, such that

$$\Delta G(B)_{FIT} = \Delta G(B)_{HLN} + F|B|, \tag{4}$$

where F is a constant that depends on the measurement temperature.

The temperature dependence of the phase coherence lengths extracted from these measurements of all three devices is shown in Figure 5. The rapid reduction in l_ϕ is consistent with the presence of electron-electron scattering in these epilayers. It is also of note that the phase coherence length is larger in the n-type epilayers than the p-type for all temperatures. The phase coherence length is greater for the n-type device with the greater carrier density. This is consistent

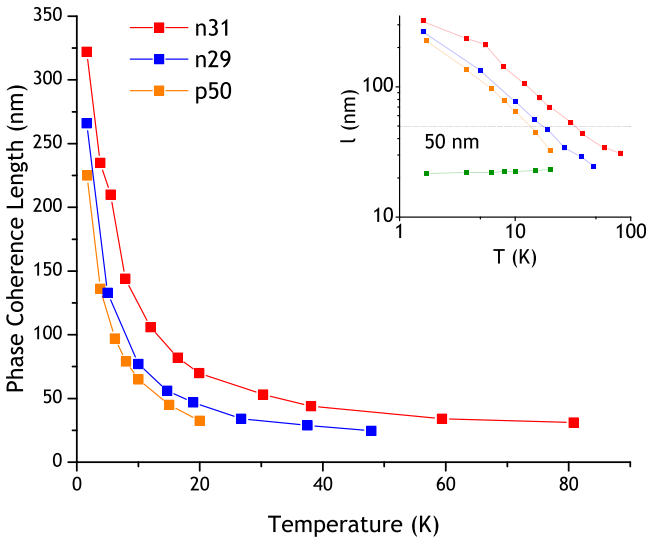

FIG. 5. Temperature variation of the phase coherence length in the n-type and p-type epilayer Hall bar devices. The inset shows the same data, displayed on a logarithmic scale. The dotted line indicates the thickness of the epilayers. The temperature variation of l_{sf} for sample p50 is included in green for comparison.

with the previous measurements of weak localization in other material systems, where the phase coherence length is enhanced by increasing the carrier density in a system.[24,25]

The inset of this graph shows the same data where both axes have logarithmic scales. Here, it can be seen that, in the region where the phase coherence length is greater than the thickness of the epilayer (indicated with a dotted line), the decay with temperature of l_ϕ is approximately the same in each device, despite the strong differences in the carrier density of the samples. Fits to these data result in a power law relationship, $l_\phi = AT^c$, where $c = -0.68 \pm 0.03$ for each device and A is a constant that depends on the sample that is measured. At temperatures where l_ϕ is smaller than the epilayer thickness, there is a deviation from this trend, suggesting a crossover towards a three dimensional system.

The low temperature phase coherence length of 325 nm found here is significantly longer than has been extracted from the previous measurements of weak antilocalization in p-type germanium epilayers.[19] This is likely to be a result of the higher mobility in the device measured in this work. As might be expected, this phase coherence length is much shorter than obtained in high mobility p-Ge quantum well devices[3] but is sufficiently large that quantum devices could be constructed to exploit these properties.

The use of Equation (2) for our fits to the weak antilocalization data allows us to extract the spin diffusion length of the p-type epilayers. Since $l_{sf} = \frac{\sqrt{3}}{2} l_{SO}$, we obtain a value of $l_{sf} = 20$ nm that shows little variation with temperature (see the inset of Figure 5). This result is similar to that obtained by Rortais *et al.* in a device with a very similar carrier density.[19] We are unable to extract a corresponding spin diffusion length for the n-type devices.

The observation of weak antilocalization implies that there is a strong spin-orbit coupling present in these p-type epilayers. The spin diffusion length, whilst small at $l_{sf} = 20$ nm, is larger than the 14 nm feature size of modern finFETs,[26] suggesting that an efficient spintronic device could be manufactured if the epilayers were optimised further and appropriate spin injection and detection contacts could be developed. Work also needs to be performed to optimise the thickness of the epilayer such that it might be possible to exploit this spin-orbit coupling using a gate field and an interfacial Rashba effect.

Over the temperature range where weak antilocalization is observed in sample p50, the spin diffusion length is approximately constant. This is consistent with momentum scattering being dominated by impurities, as would be expected at low temperature in a degenerate semiconductor in the Elliott-Yafet spin relaxation scheme.[27] The transition to phonon dominated scattering at higher temperatures cannot be observed here, owing to the rapid temperature decay in the magnitude of the weak antilocalization effect.

The presence of weak antilocalization in these p-type magnetoresistance data can also inform the analysis of the results of magnetotransport experiments on germanium quantum wells. In devices exhibiting parallel conduction, the observation of weak antilocalization has been attributed to the Rashba effect in the quantum well,[15] although the effect is reduced when devices are constructed that do not parallel conduct[3] and the thermal energy should be sufficient to obscure any spin-splitting without much greater doping densities.[4,28] Attributing this Rashba effect to transport through the highly-doped supply layer could explain this discrepancy as well as the unexpected temperature dependence of the phenomenon, where the weak antilocalization appears to vanish at the lowest measurement temperatures.

In conclusion, we have measured the magnetoresistance of both the n-type and p-type epilayers of germanium. We have performed fits to the observed weak localization and weak antilocalization using the HLN model. Phase coherence lengths as large as 325 nm were extracted using these methods, presenting possible applications in quantum technologies. The p-type spin diffusion length of 20 nm suggests that, with further optimisation, these epilayers could find use in future spintronic devices.

This work was supported by the EPSRC funded "Spintronic device physics in Si/Ge heterostructures" EP/J003263/1 and EP/J003638/1 projects and a Platform Grant No. EP/J001074/1. Additional data relevant to this publication can be found at https://doi.org/10.17863/CAM.7415.

[1]C. Shen, T. Trypiniotis, K. Y. Lee, S. N. Holmes, R. Mansell, M. Husain, V. Shah, H. Kurebayashi, I. Farrer, C. H. deGroot, D. R. Leadley, G. Bell, E. H. C. Parker, T. Whall, D. A. Ritchie, and C. H. W. Barnes, Appl. Phys. Lett. **97**, 162104 (2010).
[2]Y. Fujita, M. Yamada, S. Yamada, T. Kanashima, K. Sawano, and K. Hamaya, Phys. Rev. B **94**, 245302 (2016).
[3]P. J. Newton, J. Llandro, R. Mansell, S. N. Holmes, C. Morrison, J. Foronda, M. Myronov, D. R. Leadley, and C. H. W. Barnes, Appl. Phys. Lett. **106**, 172102 (2015).
[4]S. N. Holmes, P. J. Newton, J. Llandro, R. Mansell, C. H. W. Barnes, C. Morrison, and M. Myronov, J. Appl. Phys. **120**, 085702 (2016).
[5]Y. Zhou, W. Han, L.-T. Chang, F. Xiu, M. Wang, M. Oehme, I. A. Fischer, J. Schulze, R. K. Kawakami, and K. L. Wang, Phys. Rev. B **84**, 125323 (2011).
[6]Y. Hu, H. O. H. Churchill, D. J. Reilly, Jie Xiang, C. M. Lieber, and C. M. Marcus, Nat. Nanotechnol. **2**, 622 (2007).
[7]H. Saito, S. Watanabe, Y. Mineno, S. Sharma, R. Jansen, S. Yuasa, and K. Ando, Solid State Commun. **151**, 1159 (2011).
[8]A. Jain, J.-C. Rojas-Sanchez, M. Cubukcu, J. Peiro, J. C. Le Breton, E. Prestat, C. Vergnaud, L. Louahadj, C. Portemont, C. Ducruet, V. Baltz, A. Barski, P. Bayle-Guillemaud, L. Vila, J.-P. Attané, E. Augendre, G. Desfonds, S. Gambarelli, H. Jaffrès, J.-M. George, and M. Jamet, Phys. Rev. Lett. **109**, 106603 (2012).
[9]F. Pezzoli, F. Bottegoni, D. Trivedi, F. Ciccacci, A. Giorgioni, P. Li, S. Cecchi, E. Grilli, Y. Song, M. Guzzi, H. Dery, and G. Isella, Phys. Rev. Lett. **108**, 156603 (2012).
[10]C. Payette, K. Wang, P. J. Koppinen, Y. Dovzhenko, J. C. Sturm, and J. R. Petta, Appl. Phys. Lett. **100**, 043508 (2012).
[11]S. Dushenko, M. Koike, Y. Ando, T. Shinjo, M. Myronov, and M. Shiraishi, Phys. Rev. Lett. **114**, 196602 (2015).
[12]E. Yablonovitch, H. W. Jiang, H. Kosaka, H. D. Robinson, D. S. Rao, and T. Szkopek, Proc IEEE **91**, 761 (2003).
[13]E. J. Loren, J. Rioux, C. Lange, J. E. Sipe, H. M. van Driel, and A. L. Smirl, Phys. Rev. B **84**, 214307 (2011).
[14]C. Guite and V. Venkataraman, Appl. Phys. Lett. **101**, 252404 (2012).
[15]J. Foronda, C. Morrison, J. E. Halpin, S. D. Rhead, and M. Myronov, J. Phys.: Condens. Matter **27**, 022201 (2015).
[16]C. Morrison, C. Casteleiro, D. R. Leadley, and M. Myronov, Appl. Phys. Lett. **109**, 102103 (2016).
[17]S. Datta and B. Das, Appl. Phys. Lett. **56**, 665–667 (1990).
[18]S. Hikami, A. I. Larkin, and Y. Nagaoka, Prog. Theor. Phys. **63**, 707–710 (1980).
[19]F. Rortais, S. Oyarzún, F. Bottegoni, J.-C. Rojas-Sánchez, P. Laczkowski, A. Ferrari, C. Vergnaud, C. Ducruet, C. Beigné, N. Reyren, A. Marty, J.-P. Attané, L. Vila, S. Gambarelli, J. Widiez, F. Ciccacci, H. Jaffrès, J.-M. George, and M. Jamet, J. Phys. C **28**, 165801 (2016).

[20]N. W. Ashcroft and N. D. Mermin, *Solid State Physics* (Saunders, 1976).
[21]M. M. Parish and P. B. Littlewood, Nature **426**, 162–165 (2003).
[22]J. Chen, H.-G. Piao, Z. Luo, and X. Zhang, Appl. Phys. Lett. **106**, 173503 (2015).
[23]S. Ghosh, D. Leonhardt, and S. M. Han, J. Appl. Phys. **115**, 094507 (2014).
[24]D. J. Bishop, R. C. Dynes, and D. C. Tsui, Phys. Rev. B **26**, 773–779 (1982).
[25]E. M. Likovich, K J. Russell, E. W. Petersen, and V. Narayanamurti, Phys. Rev. B **80**, 245318 (2009).
[26]S. Natarajan, M. Agostinelli, S. Akbar, M. Bost, A. Bowonder, V. Chikarmane, S. Chouksey, A. Dasgupta, K. Fischer, Q. Fu, T. Ghani, M. Giles, S. Govindaraju, R. Grover, W. Han, D. Hanken, E. Haralson, M. Haran, M. Heckscher, R. Heussner, P. Jain, R. James, R. Jhaveri, I. Jin, H. Kam, E. Karl, C. Kenyon, M. Liu, Y. Luo, R. Mehandru, S. Morarka, L. Neiberg, P. Packan, A. Paliwal, C. Parker, P. Patel, R. Patel, C. Pelto, L. Pipes, P. Plekhanov, M. Prince, S. Rajamani, J. Sandford, B. Sell, S. Sivakumar, P. Smith, B. Song, K. Tone, T. Troeger, J. Wiedemer, M. Yang, and K. Zhang, in *2014 IEEE International Electron Devices Meeting* (2014), pp. 3.7.1–3.7.3.
[27]I. Zutic, J. Fabian, and S. Das Sarma, Rev. Mod. Phys. **76**, 323–410 (2004).
[28]R. Moriya, K. Sawano, Y. Hoshi, S. Masubuchi, Y. Shiraki, A. Wild, C. Neumann, G. Abstreiter, D. Bougeard, T. Koga, and T. Machida, Phys. Rev. Lett. **113**, 086601 (2014).